

FIELD QUALITY OF THE FERMILAB Nb₃SN COS-THETA DIPOLE MODELS*

E. Barzi, R. Carcagno, D. Chichili, J. DiMarco, H. G. Glass, V.V. Kashikhin, M. Lamm, J. Nogiec, D. Orris, T. Peterson, R. Rabehl, P. Schlabach, C. Sylvester, M. Tartaglia, J.C. Tompkins, G. Velev[†], A.V. Zlobin
 Fermilab, P.O. Box 500, Batavia, IL 60510

Abstract

Three short Nb₃Sn dipole models based on a single-bore cos-theta coil and a cold iron yoke have been fabricated and tested at Fermilab. This paper summarizes the results of magnetic measurements in those models. The geometrical harmonics, coil magnetization effects, cable eddy currents with and without a stainless steel core, and the "snap-back" effect at injection are presented.

1 INTRODUCTION

High field accelerator magnets are being developed at Fermilab for a future Very Large Hadron Collider [1]. These magnets are designed for a nominal field of 10-12 T in a magnet bore of 40-50 mm. Nb₃Sn superconductor is used in order to achieve the design fields at nominal operational temperature of 4.5 K. The magnets are based on various design approaches and fabrication techniques [2,3]. One of the design approaches being explored for these magnets is based on a two-layer cos-theta Nb₃Sn coil produced using a wind-and-react technique and a cold iron yoke. Three 1m long dipole models (HFDA02-04) based on this design were fabricated and tested in the Fermilab Vertical Magnet Test Facility. During testing, magnetic measurements were performed both warm and cold. Cold measurements were made at excitation currents up to 10 kA due restrictions imposed by magnet quench performance.

2 MAGNET DESIGN

Magnetic design and parameters of the HFDA short models are reported in [4]. Details of magnet technology and model fabrication are reported elsewhere [5]. The baseline design consists of a two-layer shell-type coil with a 43.5 mm bore and a cold iron yoke. Fig. 1 shows both a 3D view of the magnet and an assembled cold mass.

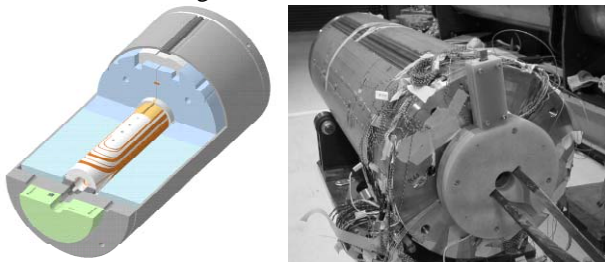


Figure 1: Short model 3D view and assembled cold mass.

The coils were wound from an unreacted keystoneed Rutherford-type cable made of 28 Nb₃Sn strands, each 1 mm in diameter. The strands were manufactured using the Modified Jelly Roll (MJR) process. Both layers of the coil were made from a single piece of cable without an interlayer splice. The cable used in HFDA02 and HFDA03 had a 25 μm thick stainless steel core to control crossover resistance while that used in HFDA04 was without the core. A 0.125 mm thick ceramic tape impregnated with liquid ceramic binder was used for cable insulation. The critical current for the virgin strand measured at 12 T and 4.2 K was in a range of 700-726 A. The critical current degradation in the magnet was less than 8.5%. Strand and cable RRR varied from 7 to 19.

Each half-coil consists of 24 turns, 11 turns in the inner layer and 13 turns in the outer layer. Two pole posts, one in the inner layer and another one in the outer layer, and four spacers per quadrant, two for each layer, minimize the low order geometrical harmonics in the magnet body. The coil ends also have a blockwise layout of turns with the same number of blocks and turns in the block as in the magnet body. Magnet ends were optimized to minimize stress in the cable blocks as well as the length of the end region.

The support structure of the models consists of a vertically split iron yoke locked by two aluminum clamps and an 8-mm thick stainless steel skin. Coil prestress is provided by clamps and skin. Aluminum spacers between the coils and the iron yoke prevent excessive compression of the coils during magnet assembly. The iron yoke has an inner diameter of 120 mm and an outer diameter of 400 mm. Two 50 mm end plates restrict longitudinal motion of coil ends under Lorentz force.

3 MEASUREMENT SYSTEM

A vertical drive rotating coil system was used for magnetic measurements. The coil used has a nominal diameter of 2.5 cm and length 25 cm. A tangential winding measures the field harmonics; dipole windings measure the main field and allowing bucking of the large dipole component in the tangential winding signal. Coil winding voltages as well as magnet current are read using HP3458 DVMs triggered simultaneously by an angular encoder on the probe shaft to synchronize measurements of field and current. A centering correction is performed using feed down of higher order allowed to lower order unallowed harmonics (18, 22 pole to 16, 20 pole).

*Work supported by the U.S. Department of Energy

[†]velev@fnal.gov

The field in the magnet body is represented in terms of harmonic coefficients defined by the power series expansion

$$B_y + iB_x = B_1 \times 10^{-4} \sum_{n=1}^{\infty} (b_n + ia_n) \left(\frac{x + iy}{r_0} \right)^{n-1},$$

where B_x and B_y are the transverse field components, B_1 is the dipole field strength, and b_n and a_n are the $2n$ -pole coefficients ($b_1=10^4$) at a reference radius r_0 of 10 mm.

A Cartesian coordinate system is defined with the z -axis at the center of the magnet aperture and pointing from return to lead end, the x -axis horizontal and pointing to the right of an observer who faces the magnet from the lead end, and the y -axis pointing upwards.

4 MEASUREMENT RESULTS

The models were tested in boiling liquid helium at 4.5 K. Quench performance of the three magnets was very similar. The maximum current achieved was ~ 10 kA, a factor of two smaller than the expected magnet critical current. All quenches in the magnets occurred in the Nb₃Sn coil leads near their splices with the flexible NbTi/copper leads. Possible causes of the observed quench performance are being studied. The low quench current reached in the magnet restricted magnetic measurements to fields up to 6 T.

4.1 Harmonics in the magnet body

The geometrical harmonics measured at 3 kA in the magnet body and calculated for the baseline design geometry are presented in Table I. The as-built coil geometry varied from magnet to magnet in order to compensate for the deviations of magnet parts from the nominal sizes and to achieve the target coil prestress. However, some improvement in the field quality of HFDA03 and HFDA04 with respect to HFDA02 can be seen. This was achieved by optimizing the coil reaction, impregnation and yoking procedures and tooling. Although some of the low order harmonics are large with respect to the RMS field errors predicted for 50 μ m coil block displacements and need to be improved, it is clear that the requirements for VLHC field quality [1] could be achieved with these magnets.

Table I: Geometrical harmonics in magnet body (I=3000A)

n	Design values		HFDA02		HFDA03		HFDA04	
	$\sigma_{an,bn}$	b_n	a_n	b_n	a_n	b_n	a_n	b_n
2	1.20	-	-9.6	4.1	1.93	-7.13	12.56	0.75
3	0.56	0.00	-0.2	-4.0	0.81	-2.36	-0.25	8.28
4	0.28	-	-1.1	0.4	-0.75	-0.19	0.06	0.16
5	0.10	0.00	0.3	0.0	0.04	-0.53	0.11	-0.34
6	0.05	-	0.3	0.0	0.03	0.12	-0.01	0.02
7	0.02	0.00	-0.1	0.1	0.03	0.04	-0.03	0.49
8	0.01	-	used for the centering correction					
9	0.00	-0.09	-0.2	-0.2	0.04	-0.01	-0.07	-0.15

4.2 Coil magnetization and its correction

The effect of coil magnetization on the normal sextupole measured and calculated in these magnets is shown in Fig. 2. Calculations of the magnetization harmonics reproduce the measured values over a wide range of measurement currents. The width of the sextupole hysteresis loop is large due to the high critical current density and large effective filament diameter that exceeds at present time 100 μ m in Nb₃Sn strands produced using the MJR process [6].

To reduce the coil magnetization effect in Nb₃Sn accelerator magnets, simple passive correctors based on thin iron strips were proposed [7]. HFDA02 and HFDA03 were tested without and with simple models of such a corrector. The correctors had four 15.85 mm wide and 0.2 mm thick iron strips placed between two layers of epoxy impregnated fiberglass tape, wrapped on a mandrell and then cured. The G10 tube thus produced was installed in the magnet bore with the iron strips at a radius of 21.4 mm. Measured and calculated sextupole loops without and with passive correction are presented in Fig. 2. It can be seen that the passive correction has effectively reduced the sextupole variation between 1.5 and 4 T on the upramp from 19.4 to 3.2 units. In fact, the corrected sextupole curve is virtually flat above 2 T field. Excellent correlation of the calculations with the measurements validates the possibility of precise prediction and correction of the coil magnetization effect in Nb₃Sn accelerator magnets.

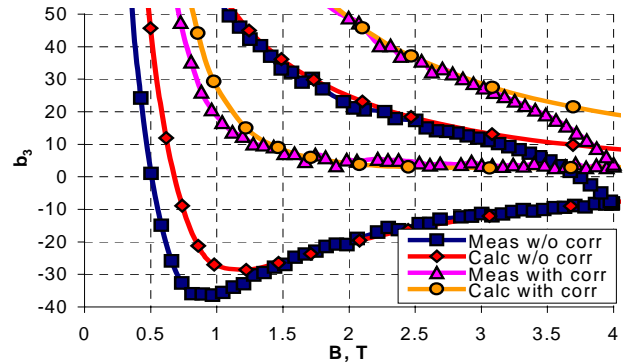


Figure 2: Normal sextupole before and after correction.

4.3 Harmonics decay and “snapback”

To check for dynamic effects during injection, measurements were performed at a current plateau of 1.75 and 3 kA for up to 30 minutes. The plateau was preceded by one or two conditioning cycles in which the magnet was ramped to maximum current. The time dependence of the normal sextupole at the injection plateau for HFDA02, 03 and 04 is presented in Fig. 3. Changes in the harmonics at current plateau are very small (<1 unit or $<2\%$) with respect to those observed in NbTi accelerator magnets. A small “oscillation” was observed in HGQ03 and HGQ04 and has yet to be understood.

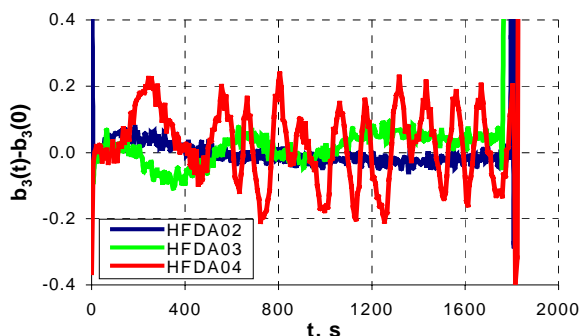


Figure 3: Time dependence of b_3 at the injection plateau. The current ramp stops at $t=0$. The first few measurements after resuming ramping are also plotted.

4.4 Cable eddy current effect

Nb_3Sn magnets fabricated using the wind-and-react technique typically show large eddy current effects due to the small crossover resistance in the cable created during coil reaction. To increase the crossover resistance in HFDA02 and 03 a thin stainless core in the cable was used. For comparison, the HFDA04 cable was made without the stainless steel core. However, it can be seen from the measured normal sextupole (Fig. 4) that the eddy current effect in all the models is small. The same is true of all the low-order allowed harmonics. It is also consistent with the results of AC loss measurements shown in Fig. 5. Apparently, the high interstrand resistance seen in all the models is related to the use of a liquid ceramic binder during the cable insulation and coil curing. This creates thin ceramic barriers on strand surfaces effectively suppressing eddy current effects even without a resistive core in the cable.

5 CONCLUSIONS

The third of three nearly identical Nb_3Sn dipole short models was fabricated and recently tested at Fermilab. Improvements of the coil end design and the lead splicing

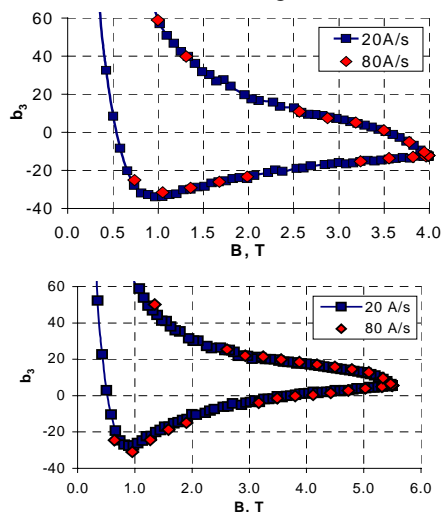


Figure 4: Normal sextupole measured at different ramp rates for HFDA03 (top) and HFDA04 (bottom).

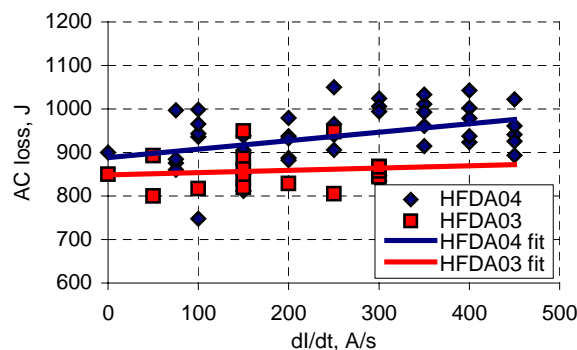


Figure 5: AC loss measured in 500-6500-500 A cycles with different current ramp rates.

technique implemented in HFDA04 have not resulted in an improvement of the magnet quench performance observed in first two models [8].

Field quality measurements of the models are consistent with expectations. Large low-order geometrical harmonics are related to the deviation of coil geometry from the design. Further improvements will be achieved by modifying the coil fabrication tooling and procedures. The relatively large measured magnetization harmonics are consistent with calculations based on the properties of Nb_3Sn strand used in these models. A scheme to minimize this effect with passive correction shims was successfully tested. Field decay and “snapback” effects in low-order allowed harmonics are small. The lack of a stainless steel core in the cable used for the last magnet did not cause large eddy current effects. Further fabrication and tests of models in this design series will be continued.

6 REFERENCES

- [1] “Design study for a Staged Very Large Hadron Collider”, Fermilab-TM-2149, June 2001.
- [2] A.V. Zlobin et al., “Development of Cos-theta Nb_3Sn Dipole Magnets for VLHC”, PAC2001, Chicago, IL June 2001.
- [3] G. Ambrosio et al., “Design and Development of Single-Layer Common Coil Nb_3Sn Dipole Magnet for VLHC”, PAC2001, Chicago, IL, June 2001.
- [4] G. Ambrosio et al., “Magnetic Design of the Fermilab 11 T Nb_3Sn Short Dipole Model”, IEEE Trans. Appl. Supercond., Vol. 10, No. 1, Mar. 2000.
- [5] D.R. Chichili et al., “Fabrication of the Shell-Type Nb_3Sn Dipole Model at Fermilab”, IEEE Trans. Appl. Supercond., Vol. 11, No. 1, Mar. 2001.
- [6] E. Barzi et al., “Study of Nb_3Sn Strands for Fermilab’s High Field Dipole Models”, IEEE Trans. Appl. Supercond., Vol. 11, No. 1, Mar. 2001.
- [7] V.V. Kashikhin and A.V. Zlobin, “Correction of the Persistent Current Effect in Nb_3Sn Dipole Magnets”, IEEE Trans. Appl. Supercond., Vol. 11, No. 1, Mar. 2001.
- [8] N. Andreev et al., “Development and Test of Single-bore Cos-theta Nb_3Sn Dipole Models with Cold Iron Yoke”, MT-17, Geneva, Switzerland, Sept. 2001.